

## Establishing empirical relationships to predict grain size and tensile strength of friction stir welded AA 6061-T6 aluminium alloy joints

S. RAJAKUMAR, C. MURALIDHARAN, V. BALASUBRAMANIAN

Department of Manufacturing Engineering, Annamalai University,  
Annamalainagar – 608 002, Chidambaram, Tamil Nadu, India

Received 21 December 2009; accepted 23 March 2010

**Abstract:** AA 6061-T6 aluminium alloy (Al-Mg-Si alloy) has gathered wide acceptance in the fabrication of light weight structures requiring a high specific strength and good corrosion resistance. Compared with the fusion welding processes that are routinely used for joining structural aluminium alloys, friction stir welding (FSW) process is an emerging solid state joining process in which the material welded does not melt and recast. Joint strength is influenced by the grain size and tensile strength of the weld nugget region. Hence, an attempt was made to develop empirical relationships to predict grain size and tensile strength of friction stir welded AA 6061-T6 aluminium alloy joints. The empirical relationships are developed by response surface methodology (RSM) incorporating FSW tool and process parameters. A linear regression relationship was also established between grain size and tensile strength of the weld nugget of FSW joints.

**Key words:** AA 6061-T6 alloy; friction stir welding; analysis of variance; regression analysis; grain size; tensile strength

### 1 Introduction

Heat treatable wrought aluminium-magnesium-silicon alloys conforming to AA 6061-T6 are of moderate strength and possess excellent welding characteristics over the high strength aluminium alloys[1]. Hence, alloys of this class are extensively employed in marine frames, pipelines, storage tanks and aircraft applications. Low distortion, high quality, lower residual stresses, fewer weld defects, and low cost joints are the main advantages of this method. The mechanical properties of the joints mainly depend on the welding parameters such as pin rotation speed, traverse speed and stirrer geometry. In order to increase the welding efficiency, mechanical properties of joints must be maximized and the defects must be minimized in the friction stir welding (FSW) process. Therefore, studying the mechanical properties and related significant factors would be effective to enhance the welding productivity and process reliability.

Recently, modeling the FSW process with different approaches is the main interest of many researchers. A series of investigations have been conducted on

modeling the FSW process with different approaches. OKUYUCU et al[2] used the artificial neural networks (ANNs) for the calculation of the mechanical properties of welded Al plates using FSW method. It was found that the correlations between the measured and predicted values of tensile strength, hardness of heat-affected zone (HAZ), and hardness of weld metal were better than those of elongation and yield strength. FRIGAARD et al[3] developed a numerical three dimensional (3D) heat flow model for FSW of AA 6082-T6 and AA 7108-T79 aluminum alloys based on the method of finite differences. ZHANG et al[4] applied the finite element method (FEM) to model the 3D material flow in FSW. The results indicated that the distribution of the equivalent plastic strain correlates well with the distribution of the microstructure zones in the weld. FERSINI and PIRONDI[5] performed an FE analysis to predict the crack path and the stress intensity factor at the crack tip and the lifetime of base material using the AFgrow software. BUFFA et al[6] proposed two different analytic models to determine the average grain size in friction stir welded AA 6061-T6 aluminum alloy joints. They developed a 3D FEM model and the numerical analyses of the welding processes have been

performed to verify their effectiveness. Same authors developed a linear regression model to predict local effects of strain, strain rate and temperature in FSW of AA 6082-T6 alloy[7].

Though extensive research has been performed to model this process, the reported research work on relating the process parameters and tool parameters to weld characteristics is very scanty. Moreover, no systematic study has been reported so far to correlate the process parameters and tool parameters with weld nugget microstructure and tensile strength. Hence, in this work, an attempt was made to develop empirical relationship to predict the grain size and tensile strength of weld nugget of friction stir welded AA 6061-T6 aluminium alloy joints using statistical tools such as design of experiments, analyses of variance and regression.

## 2 Scheme of investigation

### 2.1 Identifying important process parameters

From Refs.[7–11] and the previous work[12–13] done in our laboratory, the predominant factors that have greater influence on tensile strength of FSW process were identified. They are: 1) tool rotational speed, 2) welding (traverse) speed, 3) axial (downward) force, 4) shoulder diameter, 5) pin diameter and 6) tool hardness. These are the primary process and tool parameters contributing to the frictional heat generation and subsequently influencing the tensile properties of friction stir welded aluminium alloy joints.

### 2.2 Finding working limits of parameters

The chemical composition and mechanical properties of base metal are presented in Table 1 and 2, respectively. The microstructure of the base metal is displayed in Fig.1. Trial experiments were carried out using 5 mm-thick rolled plates of AA 6061-T6 aluminium alloy to find out the feasible working limits of FSW parameters. The working range of each parameter was decided by inspecting the macrostructure (cross section of weld) for any visible defects such as tunnel defect, pinhole, kissing bond, lazy S. From the above inspection, a few important observations were made and they are presented in Table 3. The chosen levels of important process parameters and tool parameters with their units

**Table 1** Chemical composition of base metal (mass fraction, %)

Mg	Mn	Fe	Si	Cu	Al
1.1	0.12	0.35	0.58	0.22	Bal.

**Table 2** Mechanical properties of base metal

$\sigma_{0.2}$ /MPa	$\sigma_b$ /MPa	$\delta$ /%	HV <sub>0.49N</sub>
235	283	26.4	105

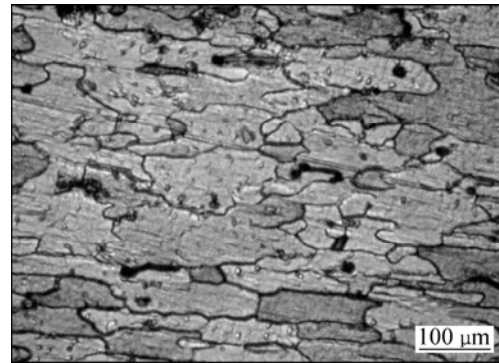


**Fig.1** Microstructure of base metal

and notations are presented in Table 4.

### 2.3 Developing experimental design matrix

By considering all the above conditions, the feasible limits of the parameters were chosen in such a way that AA 6061-T6 aluminium alloy should be welded without defects. Central composite rotatable design of second order was found to be the most efficient tool in response surface methodology (RSM) to establish the mathematical relation of the response surface using the smallest possible number of experiments without losing its accuracy[14]. Due to wide range of factors, it was decided to use six factors, five levels, central composite design matrix to optimize the experimental conditions. Table 4 presents the ranges of factors considered and Table 5 shows the 52 sets of coded conditions used to form the design matrix. First 32 experimental conditions are derived from half-factorial experimental design matrix ( $2^5=32$ ). All the variables at the intermediate (0) level constitute the center points while the combinations of each process variable at either its lowest ( $-2.378$ ) or its highest ( $+2.378$ ) with the other twelve variables of the intermediate levels constitute the start points. Thus, the 52 experimental conditions allowed the estimation of the linear, quadratic and two-way interactive effects of the variables on the tensile strength of welded joints. The method of designing such matrix is dealt elsewhere. For the convenience of recording and processing experimental data, upper and lower levels of the factors are coded as  $+2.378$  and  $-2.378$ , respectively. The coded values of intermediate values can be calculated using the following expression[15–18]:

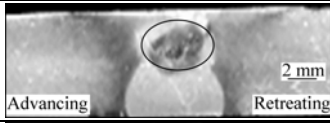
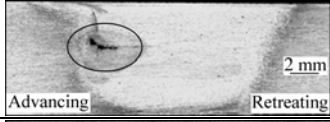
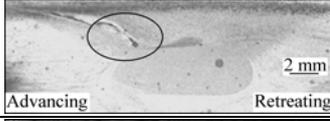
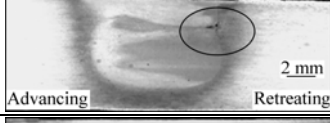
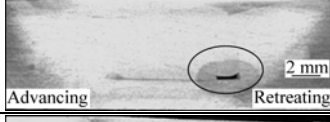
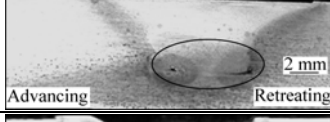
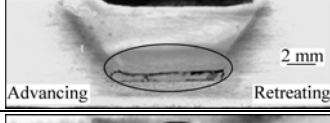
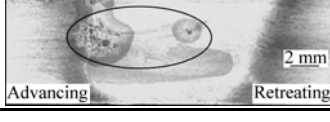
$$X_i = 2[2X - (X_{\max} + X_{\min})] / (X_{\max} - X_{\min}) \quad (1)$$

where  $X_i$  is the required coded value of a variable  $X$ ;  $X$  is any value of the variable from  $X_{\min}$  to  $X_{\max}$ ;  $X_{\min}$  is the lower level of the variable;  $X_{\max}$  is the highest level of the variable.

### 2.4 Conducting experiments and recording responses

Roller plates of medium strength aluminium

**Table 3** Macrostructure observation results of AA 6061-T6 aluminium alloy

Input parameter	Parameter range	Macrostructure	Name of defect	Probable reason
Rotational speed	<900 r/min		Tunnel defect	Insufficient heat generation and insufficient metal transportation
Rotational speed	>1 700 r/min		Pin hole	Further increase in turbulence of plasticized metal
Welding speed	<25 mm/min		Tunnel defect	Excess heat input per unit length of weld and no vertical movement of metal
Welding speed	>125 mm/min		Kissing bond	Increase in welding speed resulted in poor plasticization of metal and associated defect
Axial force	<3 kN		Tunnel hole	Insufficient axial force and inadequate heat generation
Axial force	>11 kN		Worm hole	Additional axial force leads to excess heat input and thinning of weld zone
Shoulder diameter	<9 mm		Pin hole	Insufficient stirring butt surfaces could be directly bonded without metallic bond between oxide free surfaces in root part of weld
Shoulder diameter	>21 mm		Pin hole	Excessive heat input due to softening and work hardening effect
Pin diameter	<3 mm		Piping defect	Asymptote heat generation and insufficient metal transportation
Pin diameter	>7 mm		Tunnel defect	Excessive heat input due to softening
Tool hardness	<HV300		Pin hole	Due to low frictional heat generation
Tool hardness	>HV900		Worm hole	High frictional heat generation

**Table 4** Important FSW process parameters and their levels for AA 6061-T6 aluminium alloy

Factor	Factor level				
	-2.378	-1	0	+1	+2.378
Tool rotational speed, $N/(r \cdot \text{min}^{-1})$	924	1200	1400	1600	1875
Welding speed, $S/(\text{mm} \cdot \text{min}^{-1})$	12.43	40	60	80	107.56
Axial force, $F/\text{kN}$	5.62	7	8	9	10.37
Tool shoulder diameter, $D/\text{mm}$	7.86	12	15	18	22.13
Pin diameter, $d/\text{mm}$	2.62	4	5	6	7.37
Tool hardness (HV), $N$	243	450	600	750	956

**Table 5** Experimental design matrix and results

Joint No.	Input parameter						Output response	
	$N(X_1)$	$S(X_2)$	$F(X_3)$	$D(X_4)$	$d(X_5)$	$H(X_6)$	Weld nugget grain size/ $\mu\text{m}$	Tensile strength/MPa
1	-1	-1	-1	-1	-1	-1	49.03	186
2	1	-1	-1	-1	-1	1	46.66	190
3	-1	1	-1	-1	-1	1	69.74	165
4	1	1	-1	-1	-1	-1	44.72	192
5	-1	-1	1	-1	-1	1	64.86	167
6	1	-1	1	-1	-1	-1	44.71	192
7	-1	1	1	-1	-1	-1	63.81	168
8	1	1	1	-1	-1	1	44.66	193
9	-1	-1	-1	1	-1	1	62.54	169
10	1	-1	-1	1	-1	-1	42.62	195
11	-1	1	-1	1	-1	-1	62.09	170
12	1	1	-1	1	-1	1	42.29	196
13	-1	-1	1	1	-1	-1	60.26	172
14	1	-1	1	1	-1	1	41.14	198
15	-1	1	1	1	-1	1	59.62	173
16	1	1	1	1	-1	-1	41.00	198
17	-1	-1	-1	-1	1	1	53.76	177
18	1	-1	-1	-1	1	-1	40.21	200
19	-1	1	-1	-1	1	-1	53.58	177
20	1	1	-1	-1	1	1	40.21	200
21	-1	-1	1	-1	1	-1	53.20	178
22	1	-1	1	-1	1	1	39.84	201
23	-1	1	1	-1	1	1	52.40	179
24	1	1	1	-1	1	-1	39.26	201
25	-1	-1	-1	1	1	-1	52.17	179
26	1	-1	-1	1	1	1	47.75	188
27	-1	1	-1	1	1	1	51.88	181
28	1	1	-1	1	1	-1	37.88	203
29	-1	-1	1	1	1	1	50.65	182
30	1	-1	1	1	1	-1	37.42	203
31	-1	1	1	1	1	-1	49.54	184
32	1	1	1	1	1	1	36.75	204
33	-2.378	0	0	0	0	0	70.08	164
34	2.378	0	0	0	0	0	33.80	207
35	0	-2.378	0	0	0	0	49.23	185
36	0	2.378	0	0	0	0	33.54	207
37	0	0	-2.378	0	0	0	49.21	185
38	0	0	2.378	0	0	0	33.18	208
39	0	0	0	-2.378	0	0	48.50	187
40	0	0	0	2.378	0	0	32.61	209
41	0	0	0	0	-2.378	0	47.88	188
42	0	0	0	0	2.378	0	27.60	214
43	0	0	0	0	0	-2.378	47.45	188
44	0	0	0	0	0	2.378	38.02	202
45	0	0	0	0	0	0	24.23	222
46	0	0	0	0	0	0	24.80	220
47	0	0	0	0	0	0	24.70	221
48	0	0	0	0	0	0	24.80	220
49	0	0	0	0	0	0	24.78	220
50	0	0	0	0	0	0	24.81	219
51	0	0	0	0	0	0	24.82	219
52	0	0	0	0	0	0	24.80	220

AA 6061-T6 alloy with 5 mm in thickness were cut to the required size (300 mm×150 mm) by power hacksaw cutting and milling. Square butt joint configuration (300 mm×300 mm) was prepared to fabricate FSW joints. The initial joint configuration was obtained by securing the plates in position using mechanical clamps. The direction of welding was normal to the rolling direction. Single pass welding procedure was followed to fabricate the joints. Non-consumable tools made of high carbon steel were used to fabricate the joints. The tool nomenclature is shown in Fig.2(a). Based on six factors, five level central composite designs, 15 tools were made with different pin diameters, shoulder diameters and tool hardnesses. Five levels of tool hardness were obtained by heat-treating high carbon steel in different quenching media (air, oil, water and furnace cooling). An indigenously designed and developed computer numerically controlled friction stir welding machine (22 kW, 4 000 r/min, 6 t) as shown in Figs.2(b) and (c) was used to fabricate the joints. As prescribed by the design matrix, 52 joints were fabricated and selected joints are displayed in Fig.2(d). The welded joints were sliced using a power hacksaw and then machined to the required dimensions to get tensile specimens. The tensile specimens were prepared as per the ASTM E8M-04 guidelines and the dimensions are shown in Fig.2(e). Tensile test was carried out in 100 kN, servo controlled

universal testing machine. The specimen was loaded at the rate of 1.5 kN/min as per ASTM specifications, so that tensile specimens underwent uniform deformation. The specimen finally failed after necking and the load versus displacement was recorded.

Microstructural examination was carried out using a light optical microscope (VERSAMET-3) incorporated with an image analyzing software (Clemex-Vision). The specimens for metallographic examination were sectioned to the required size from the joint comprising weld metal and base metal regions and were polished using different grades of emery papers. Final polishing was done using the diamond compound (1 μm in particle size) in the disc-polishing machine. Specimens were etched with Keller's reagent to reveal the microstructure. Some micrographs of the weld nugget region are displayed in Fig.3. A vickers microhardness testing machine (Shimadzu HMV-2T) was employed for measuring the hardness of the weld nugget region with 0.49 N load. The average grain diameter of the weld nugget region was measured by applying Heyn's line intercept method.

### 3 Developing empirical relationships

The grain size and tensile strength of the weld nugget of FSW joints are functions of rotational speed

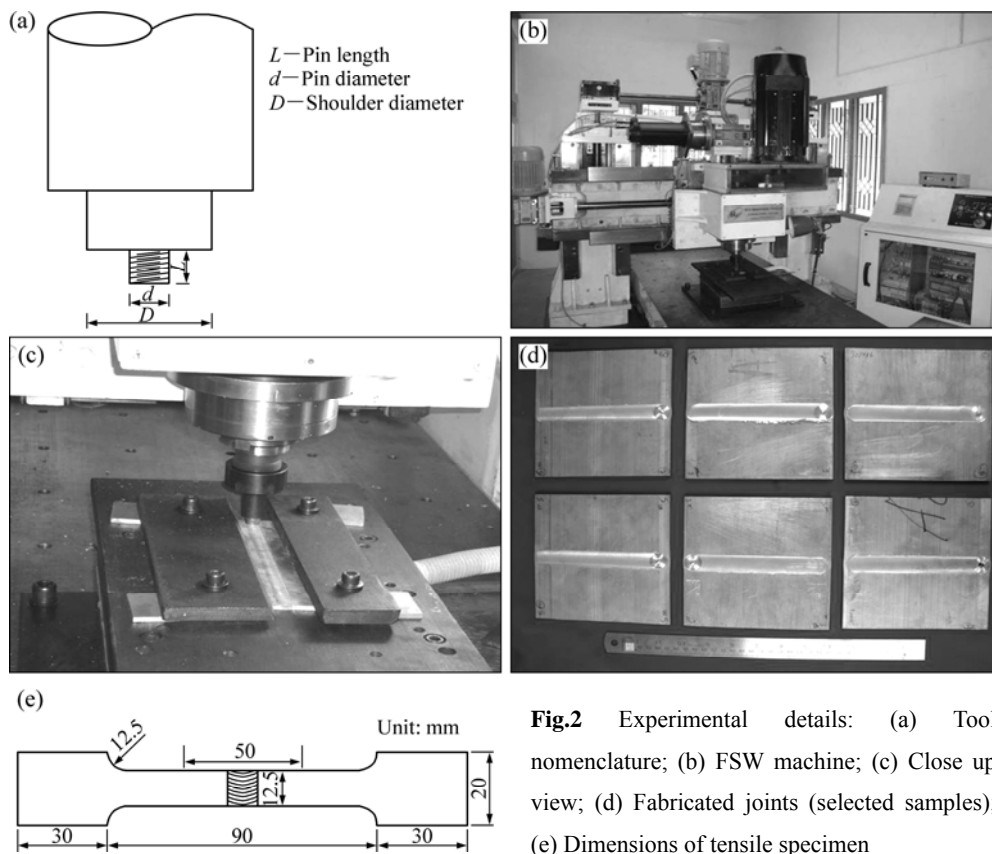


**Fig.2** Experimental details: (a) Tool nomenclature; (b) FSW machine; (c) Close up view; (d) Fabricated joints (selected samples); (e) Dimensions of tensile specimen

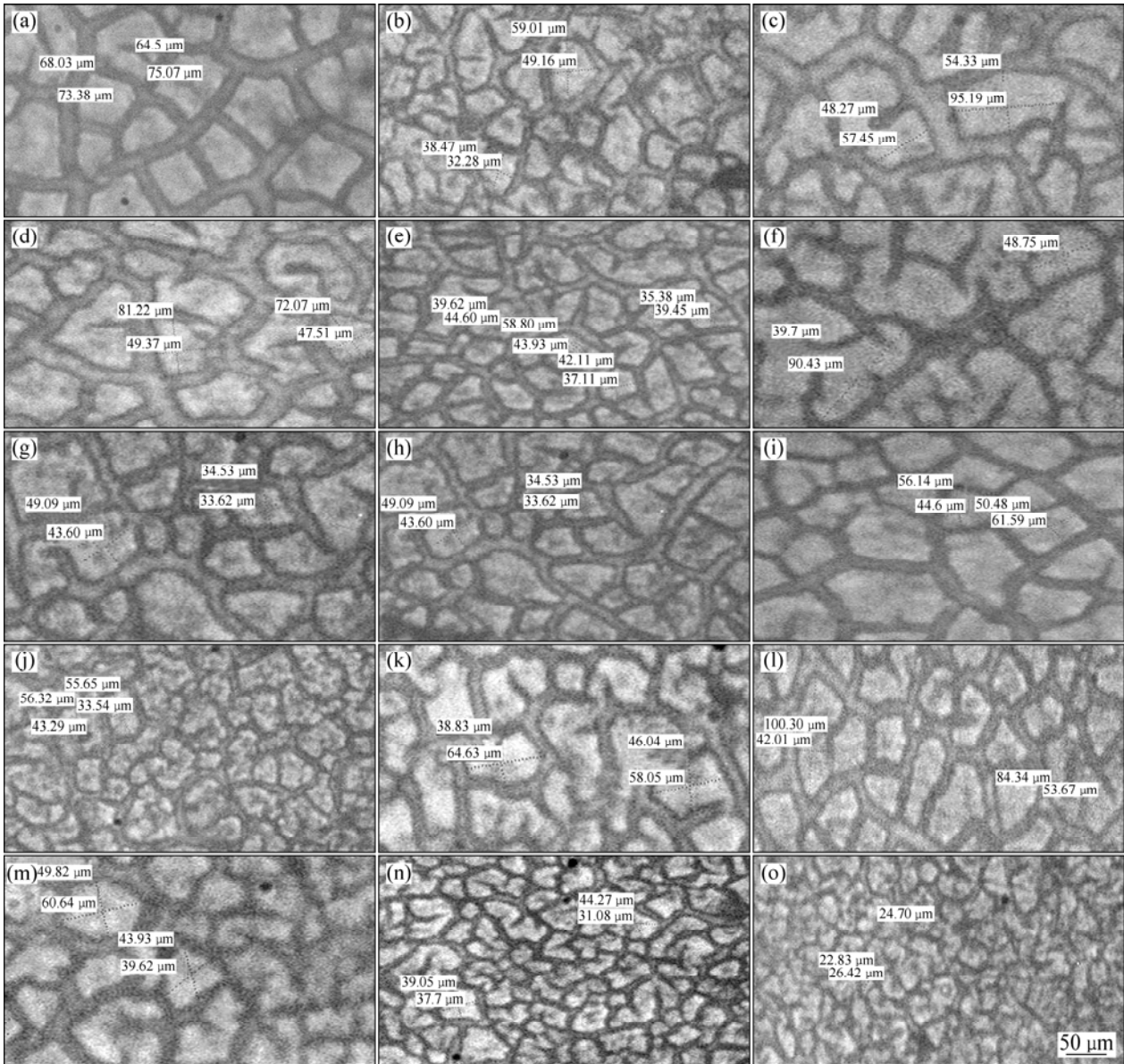


**Fig.3** Optical micrographs of weld nugget region: (a) Joint 3 ( $G_{ave}=69.74 \mu\text{m}$ ); (b) Joint 6 ( $G_{ave}=44.71 \mu\text{m}$ ); (c) Joint 7 ( $G_{ave}=63.81 \mu\text{m}$ ); (d) Joint 9 ( $G_{ave}=62.54 \mu\text{m}$ ); (e) Joint 10 ( $G_{ave}=42.62 \mu\text{m}$ ); (f) Joint 15 ( $G_{ave}=59.62 \mu\text{m}$ ); (g) Joint 18 ( $G_{ave}=40.21 \mu\text{m}$ ); (h) Joint 20 ( $G_{ave}=40.21 \mu\text{m}$ ); (i) Joint 21 ( $G_{ave}=53.20 \mu\text{m}$ ); (j) Joint 26 ( $G_{ave}=47.45 \mu\text{m}$ ); (k) Joint 27 ( $G_{ave}=51.88 \mu\text{m}$ ); (l) Joint 33 ( $G_{ave}=70.88 \mu\text{m}$ ); (m) Joint 39 ( $G_{ave}=48.50 \mu\text{m}$ ); (n) Joint 44 ( $G_{ave}=38.02 \mu\text{m}$ ); (o) Joint 45 ( $G_{ave}=24.23 \mu\text{m}$ )

( $N$ ), welding speed ( $S$ ), axial force ( $F$ ), shoulder diameter ( $D$ ), pin diameter ( $d$ ) and tool hardness ( $H$ ), and it can be expressed as[15–17]:

Weld nugget grain size

$$G=f(N, S, F, D, d, H) \tag{2}$$

Tensile strength

$$\sigma_b=f(N, S, F, D, d, H) \tag{3}$$

The second order polynomial (regression) equation used to represent the response surface ‘ $Y$ ’ is given by[19]:

$$Y=b_0+\sum b_i x_i+\sum b_{ii} x_i^2+\sum b_{ij} x_i x_j +e_r \tag{4}$$

and for 6 factors, the selected polynomial could be expressed as:

$$\begin{aligned} G \text{ or } \sigma_b = & b_0+b_1(N)+b_2(S)+b_3(F)+b_4(D)+b_5(d)+ \\ & b_6(H)+b_{11}(N^2)+b_{22}(S^2)+b_{33}(F^2)+b_{44}(D^2)+ \\ & b_{55}(d^2)+b_{66}(H^2)+b_{12}(NS)+b_{13}(NF)+b_{14}(ND)+ \\ & b_{15}(Nd)+b_{16}(NH)+b_{23}(SF)+b_{24}(SD)+b_{25}(Sd)+ \\ & b_{26}(SH)+b_{34}(FD)+b_{35}(Fd)+b_{36}(FH)+b_{45}(Dd)+ \\ & b_{46}(DH)+b_{56}(dH) \end{aligned} \tag{5}$$

where  $b_0$  is the average of responses and  $b_1, b_2, \dots, b_{66}$  are the coefficients that depend on respective main and interaction effects of the parameters. The values of the coefficients were calculated using the following expressions, and the calculated values are presented in Table 6.

**Table 6** Calculated values of coefficients

Coefficient	For weld nugget grain size	For tensile strength
$b_0$	24.380 14	220.410 3
$b_1$	-7.579 56	12.129 67
$b_2$	-0.801 3	1.369 661
$b_3$	-1.296 03	1.840 146
$b_4$	-1.450 88	1.877 584
$b_5$	-3.497 37	4.036 569
$b_6$	0.249 841	-0.039 3
$b_{11}$	-0.930 31	1.031 25
$b_{22}$	-0.534 69	0.843 75
$b_{33}$	-0.055 94	0.093 75
$b_{44}$	1.446 563	-0.656 25
$b_{55}$	-0.321 56	0.218 75
$b_{66}$	-0.396 56	0.218 75
$b_{12}$	-0.925 31	1.218 75
$b_{13}$	-0.925 31	1.093 75
$b_{14}$	-0.684 69	0.968 75
$b_{15}$	-0.864 69	1.281 25
$b_{16}$	-0.585 94	0.906 25
$b_{23}$	-0.994 06	1.156 25
$b_{24}$	0.256 562	-0.218 75
$b_{25}$	-0.436 56	0.281 25
$b_{26}$	-0.415 31	0.281 25
$b_{34}$	5.567 119	-9.587 56
$b_{35}$	3.701 241	-4.902 97
$b_{36}$	3.667 654	-4.814 59
$b_{45}$	3.554 517	-4.549 42
$b_{46}$	3.056 89	-4.019 09
$b_{56}$	3.939 89	-5.079 75

$$b_0=0.110\ 749(\sum y)-0.018\ 738\sum(X_{ij}y) \quad (6)$$

$$b_i=0.023\ 087\sum(X_{ij}y) \quad (7)$$

$$b_{ii}=0.015\ 2625\sum(X_{ij}y)+0.001\ 217\sum\sum(X_{ij}y)-0.018\ 738(\sum y) \quad (8)$$

$$b_{ij}=0.031\ 25\sum(X_{ij}y)/n \quad (9)$$

All the coefficients were tested for their significance at 95% confidence level applying Fisher's F-test using Design expert statistical software package. After determining the significant coefficients, the final models were developed incorporating only these coefficients. The final empirical relationships to estimate grain size and tensile strength of weld nugget, developed by the above procedure, are given as follows.

Weld nugget grain size:

$$G=24.38-7.57N-3.49d+5.56N^2+3.70S^2+3.66F^2+3.55D^2+3.05d^2+3.39H^2 \quad (10)$$

Tensile strength:

$$\sigma_b=220.41+12.1N+4.03d-9.58N^2-4.90S^2-4.81F^2-4.54D^2-4.01d^2-5.07H^2 \quad (11)$$

### 3.1 Testing adequacy of developed empirical relationships

The adequacy of the developed empirical relationships was tested using the analysis of variance (ANOVA) technique[20]. As per this technique, if the calculated value of the  $F$ -ratio of the developed model is less than the standard  $F$ -ratio (from  $F$ -table) value at a desired level of confidence (say 95%), then the model is said to be adequate within the confidence limit. From the response of weld nugget grain size, the "Model  $F$ -value" of 9.86 implies that the model is significant. There is only a 0.01% chance that a "Model  $F$ -value" could occur due to noise. Values of "Prob  $> F$ " less than 0.050 0 indicate that model terms are significant. In this case,  $N, d, N^2, S^2, F^2, D^2, d^2, H^2$  are significant model terms. Values greater than 0.100 0 indicate that the model terms are not significant. The "Lack of Fit  $F$ -value" of 968.90 implies the "Lack of Fit" is significant. There is only a 0.01% chance that a "Lack of Fit  $F$ -value" could occur due to noise. The "Pred  $R$ -squared" of 92.3% is in reasonable agreement with the "Adj  $R$ -squared" of 82.4%. Similarly, from the response of tensile strength, the "Model  $F$ -value" of 12.45 implies that the model is significant. There is only a 0.01% chance that a "Model  $F$ -value" could occur due to noise. Values of "Prob  $> F$ " less than 0.050 0 indicate that model terms are significant. In this case,  $N, d, N^2, S^2, F^2, D^2, d^2$  and  $H^2$  are significant model terms. Values greater than 0.100 0 indicate that the model terms are not significant. The "Lack of Fit  $F$ -value" of 69.11 implies that the "Lack of Fit" is not significant. There is only a 0.01% chance that a "Lack of Fit  $F$ -value" could occur due to noise. The "Pred  $R$ -squared" of 59% is in reasonable agreement with the "Adj  $R$ -squared" of 86%. Calculated value of the  $R$ -ratio of the developed relationships exceed the standard tabulated value of the  $R$ -ratio for a desired level of confidence (say 95%), then the relationship may be considered to be adequate within the confidence limit. ANOVA test results for both the responses are presented in Table 7. It can be understood that the developed relationships are adequate to predict the grain size and tensile strength of weld nugget of friction stir welded AA 6061-T6 aluminium alloy at 95% confidence level. Coefficient of determination ( $r^2$ ) is used to find how close the predicted and experimental values lie and it is calculated using the following expression[20]:

**Table 7** ANOVA test results

	Term	<i>G</i>	$\sigma_b$
First-order terms	Sum of squares(SS)	3 212.60	7 459.1
	Degrees of freedom(DF)	6	6
	Mean squares(MS)	535.43	1 243.18
Second-order terms	Sum of squares(SS)	7 346.36	16 263.12
	Degrees of freedom(DF)	27	27
	Mean squares(MS)	272.09	602.34
Error order terms	Sum of squares(SS)	0.28	6.87
	Degrees of freedom(DF)	7	7
	Mean squares(MS)	0.040	0.98
	Sum of squares(SS)	662.03	1153.9
Lack of fit	Degrees of freedom(DF)	17	17
	Mean squares(MS)	38.94	67.87
	$F_{ratio}$ (calculated)	968.91	12.45
	$F_{ratio}$ (from table) (27,7,0.05)	2.37	2.37
	$R_{ratio}$ (calculated)	49.4	59.4
	$R_{ratio}$ (from table) (33,7,0.05)	2.30	2.30
	Whether model is adequate?	YES	YES

$$r^2 = (\text{Explained variation}) / (\text{Total variation}) \quad (12)$$

The value of  $r^2$  for the above-developed models is found to be 92% and 93% for grain size and tensile strength, respectively, which indicates high correlation between the experimental values and predicted values and this is further supported by correlation graphs shown in Fig.4.

**3.2 Relationship between grain size and tensile strength of weld nugget**

The weld nugget grain diameter and the tensile strength obtained from the experimental results are related, as shown in Fig.5. The experimental data points are fitted by a straight line. The straight line is governed by the following regression equation:

$$\sigma_b = 252.4 - 1.339G \quad (13)$$

The slope of the estimated regression equation (-1.339) is negative, implying that as grain size increases, the tensile strength decreases. The coefficient of determination is  $R^2=98.8\%$ , which can be interpreted as the percentage of the total sum of squares that can be explained by using the estimated regression equation. In other words, 98.8% of the variability in tensile strength can be explained by the linear relationship between the weld nugget grain size and tensile strength and it is presented in Table 8. The coefficient of determination  $R^2$  is a measure of the goodness of fit of the estimated regression equation[21–22]. The fitted regression line (Eq.(13)) may be used for two purposes: 1) estimating the mean value of tensile strength for the given value of Weld nugget grain diameter; and 2) predicting an

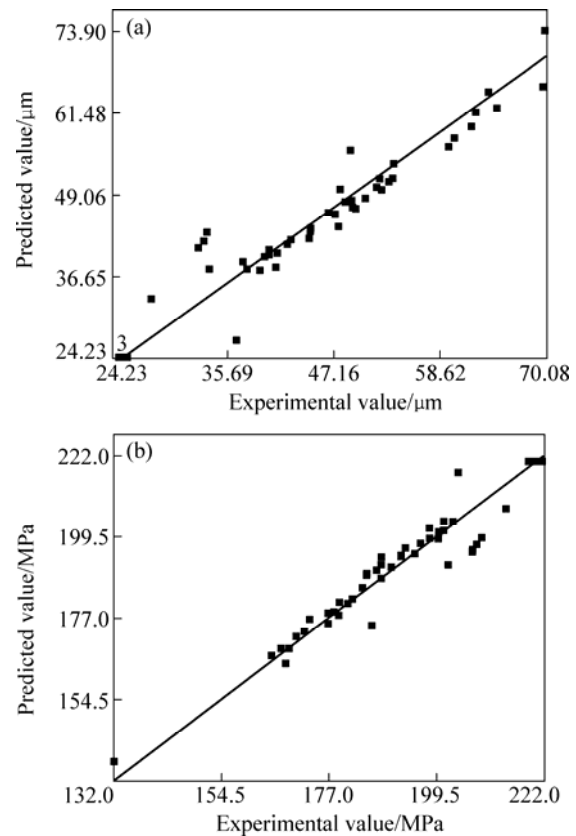


**Fig.4** Correlation graphs for responses: (a) Weld nugget grain size; (b) Tensile strength

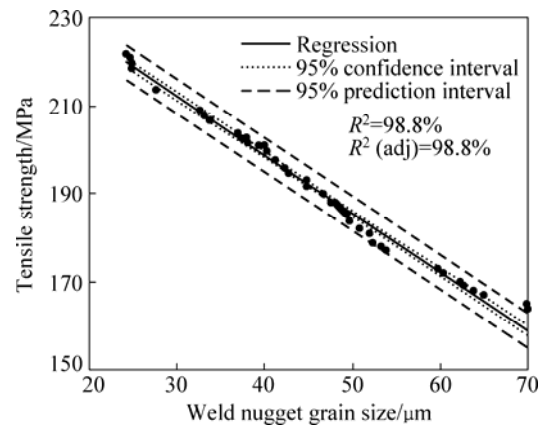


**Fig.5** Relationship between weld tensile strength and weld nugget grain size

**Table 8** Analysis of variance test result for linear regression model (Eq.(13))

Source	DF	SS	MS	F	P
Regression	1	14 352	14 352	4 111.21	0
Error	50	175	3		
Total	51	14527			

$R^2=98.8\%$   
 $R^2(\text{adj})=98.8\%$

SS—Sum of squares; DF—Degrees of freedom; MS—Mean square; F—Fishers t-test; P—Probability.

**Table 9** CI and PI for predicting tensile strength

Actual value		Predicted value				
Weld nugget grain size/ $\mu\text{m}$	Fit	Standard error fit	95%CI		95%PI	
			Low	High	Low	High
40 (near $\bar{x}$ )	198.857	0.272	198.311	199.403	195.06	202.65
45 (away from $\bar{x}$ )	179.14	9.47	160.13	198.15	382.73	319.54

CI—Confidence interval; PI—Prediction interval

individual value of tensile strength for a given value of weld nugget grain diameter.

The confidence interval (CI) and prediction interval (PI) show the precision of the regression results. Narrower intervals provide a higher degree of precision (Fig.5). Confidence interval is an interval estimate of the mean value of  $y$  for a given value of  $x$ . Prediction interval is an interval estimate of an individual value of  $y$  for a given value of  $x$ . The estimated regression equation provides a point estimate of the mean value of tensile strength for a given value of grain size. The difference between CI and PI reflects the fact that it is possible to estimate the mean value of tensile strength more precisely than an individual value. The greater width of the PI reflects the added variability introduced by predicting a value of the random variable as opposed to estimating a mean value. From Table 9, it is also inferred that the closer the value to  $\bar{x}$  (43.9  $\mu\text{m}$ ), the narrower the interval will be.

## 4 Conclusions

1) Empirical relationships were developed to estimate the average grain size and tensile strength of weld nugget of friction stir welded AA 6061-T6 aluminium alloy joints incorporating FSW tool and process parameters.

2) A linear regression equation was established between grain size and tensile strength of the weld nugget of friction stir welded AA 6061-T6 aluminium alloy joints.

3) The developed relationships can be effectively used to predict the grain size and tensile strength of friction stir welded AA 6061-T6 aluminium alloy joints within the range of parameters.

## Acknowledgements

The authors are grateful to the Department of Manufacturing Engineering, Annamalai University, Annamalai Nagar, India, for extending the facilities of Material Testing Laboratory to carry out this investigation. The authors wish to place their sincere thanks to Clean Technology Division of Ministry of Environment and Forest, Government of India, New Delhi, for financial support rendered through a R&D

Project No. MoEF1-9/2005-CT. Authors would like to thank Mr. E. BALAMURUGAN, post graduate student, Mr. K. SUBRAMANIYAN, senior foreman, Manufacturing Engineering, Mr. S. MUTHUKUMARAN, Mr. N. SAIRAMAN and Mr. A. K. THILLAIPARAMAN of project assistants, CEMAJOR for their help and support.

## References

- [1] THOMAS W M. Friction stir welding. International Patent Application No. PCT/GB92/02203, GB Patent Application No. 9125978.8, U.S. Patent No.5,460,317[P]. 1991.
- [2] OKUYUCU H, KURT A, ARCAKLIOGLU E. Artificial neural network application to the friction stir welding of aluminum plates [J]. Materials and Design, 2007, 28: 78–84.
- [3] FRIGAARD O, GRONG O, MIDLING O T. A process model for friction stir welding of age hardening aluminum alloys [J]. Metallurgical and Materials Transactions A, 2001, 32: 1189–1200.
- [4] ZHANG H W, ZHANG Z, CHEN J T. 3D modeling of material flow in friction stir welding under different process parameters [J]. Materials Processing Technology, 2007, 183: 62–70.
- [5] FERSINI D, PIRONDI A. Analysis and modeling of fatigue failure of friction stir welded aluminum alloy single-lap joints [J]. Engineering Fracture Mechanics, 2008, 75: 790–803.
- [6] BUFFA G, FRATINI L, SHIVPURI R. CDRX modeling in friction stir welding of AA 7075-T6 aluminum alloy: Analytical approaches [J]. Materials Processing Technology, 2007, 191: 356–359.
- [7] FRATINI L, BUFFA G. CDRX modeling in friction stir welding of aluminum alloys[J]. Int Machine Tools and Manufacture, 2005, 45: 1188–1194.
- [8] THOMAS W M, NICHOLAS E D. Friction stir welding for the transportation industries [J]. Materials and Design, 1997, 18: 269–273.
- [9] OOSTERKAMP A, DJAPIC OOSTERKAMP L, NORDEIDE A. Kissing bond phenomena in solid state welds of aluminium alloys [J]. Welding, 2004: 225–231.
- [10] ZENG W M, WU H L, ZHANG J. Effect of tool wear on microstructure, mechanical properties and acoustic emission of friction stir welded 6061 Al alloy [J]. Acta Metallurgica Sinica, 2006, 19(1): 9–19.
- [11] OLGA V F. The influence of pin geometry on bonding and mechanical properties in friction stir weld 2014 Al alloy [J]. Scripta Materialia, 1998, 38(5): 703–708.
- [12] ELANGO VAN K, BALASUBRAMANIAN V. Influences of tool pin profile and tool shoulder diameter on the formation of friction stir processing zone in AA6061 aluminium alloy [J]. Materials and Design, 2008, 29: 362–373.
- [13] ELANGO VAN K, BALASUBRAMANIAN V, BABU S. Predicting tensile strength of friction stir welded AA6061 aluminium alloy joints by a mathematical model [J]. Materials and Design, 2009, 30: 188–193.

- [14] GUNARAJ V, MURUGAN N. Application of response surface methodology for predicting weld bead quality in submerged arc welding of pipes [J]. *Materials Processing Technology*, 1999, 88: 266–275
- [15] COCHRAN W G, COX G M. *Experimental designs* [M]. London: John Wiley & Sons Inc, 1957.
- [16] BARKER T B. *Quality by experimental design* [M]. Marcel Dekker: ASQC Quality Press, 1985.
- [17] GARDINER W P, GETTINBY G. *Experimental design techniques in statistical practice* [M]. Chichester: Horwood Press, 1998.
- [18] RAJAKUMAR S, MURALIDHARAN C, BALASUBRAMANIAN V. Optimization of the friction-stir- welding process and the tool parameters to attain a maximum tensile strength of AA7075-T6 aluminium alloy [J]. *Journal of Engineering Manufacture*, 2010, 224: 1175–1191.
- [19] SENTHIL KUMAR T, BALASUBRAMANIAN V, SANAVULLAH M Y. Influences of pulsed current tungsten inert gas welding parameters on the tensile properties of AA 6061 aluminium alloy [J]. *Materials and Design*, 2007, 28: 2080–2092.
- [20] MILLER J E, FREUND, JOHNSON R. *Probability and statistics for engineers* [M]. New Delhi: Prentice Hall, 1996.
- [21] CANGELOSI V E, TAYLOR P H, RICE P F. *Basic statistics: A real world approach* [M]. 3rd ed. St. Paul, Minnesota: West Publishing Company, 1983: 315–364.
- [22] MONTGOMERY D C, HUNGER G C. *Applied probability for engineers* [M]. London: John Wiley & Sons Inc, 1994: 471–529.

(Edited by YANG Bing)